N-Methyl-D-Aspartate Receptor Type 2B Is Epigenetically Inactivated and Exhibits Tumor-Suppressive Activity in Human Esophageal Cancer

Myoung Sook Kim,[1] Keishi Yamashita,[1] Jin Hyen Baek,[2] Hannah Lui Park,[1] Andre Lopes Carvalho,[1] Motonobu Osada,[1] Mohammad Obaidul Hoque,[1] Sunil Upadhyay,[1] Masaki Mori,[3] Chulso Moon,[1] and David Sidransky[1]

[1]Department of Otolaryngology, Head and Neck Cancer Research Division and [2]Department of Genetic Medicine, Institute of Cell Engineering, Johns Hopkins University School of Medicine, Baltimore, Maryland and [3]Department of Surgical Oncology, Medical Institute of Bioregulation, Kyushu University, Beppu, Japan

Abstract

Promoter hypermethylation accompanied by gene silencing is a common feature of human cancers. We identified previously several new tumor suppressor genes based on pharmacologic unmasking of the promoter region and detection of reexpression on microarray analysis. In this study, we modified the selection of candidates from our previous microarray data by excluding genes that showed basal expression in cancer cell lines. With the new method, we found novel methylated genes with 90% accuracy. Among these 33 novel methylated genes that we identified in esophageal squamous cell carcinoma (ESCC) cell lines, *N*-methyl-D-aspartate receptor type 2B (*NMDAR2B*) was of particular interest. *NMDAR2B* was methylated in 95% of primary human ESCC tissue specimens and 12 ESCC cell lines by sequence analysis. *NMDAR2B* expression was silenced in all 12 ESCC cell lines and was reactivated by the demethylating agent 5-aza-2′-deoxycytidine. Moreover, reintroduction of the gene was accompanied by marked Ca^{2+}-independent apoptosis in ESCC cell lines, suggesting that *NMDAR2B* can suppress tumor growth. Thus, *NMDAR2B* promoter methylation is common in ESCC, abrogating gene transcription and leading to cellular resistance to apoptosis. (Cancer Res 2006; 66(7): 3409-18)

Introduction

Hypermethylated DNA associates with *MeCP2* protein, which recruits histone deacetylase (*HDAC*), resulting in formation of condensed chromatin and gene silencing (1, 2). Aberrant methylation of DNA promoters in primary cancers includes hypermethylation of tumor suppressor genes (TSG; ref. 3) and hypomethylation of oncogenic molecules (4, 5). DNA hypermethylation is a common mechanism in inactivating TSGs through shutdown of gene expression (3). Pharmacologic unmasking using a demethylating agent 5-aza-2′-deoxycytidine (5-Aza-dC) and a HDAC inhibitor trichostatin A (TSA) can synergistically reactivate TSGs (6). This pharmacologic unmasking results in growth arrest and inhibition of tumorigenesis *in vitro* (7) and suppression of tumors *in vivo* (8).

N-methyl-D-aspartate receptors (*NMDAR*) are the first class of glutamate receptors and the predominant excitatory neurotransmitter receptors in the mammalian brain (9). *NMDAR* family members are endogenously expressed neurotoxic molecules that can be activated in a variety of normal neurophysiologic processes (10). Functional *NMDARs* are heteromers composed of the key invariable receptor subunit (*NMDAR1*) and one or more of several variable subunits (*NMDAR2A-D, NMDAR3A,* and *NMDAR3B*), which play critical roles in spatial learning and memory (11). The classification of glutamate receptors are based on their activation by different pharmacologic agonists. NMDA and excitatory amino acids, such as glutamate or glycine, are agonists for *NMDAR* activation.

Some *NMDAR* subunits have been detected in skeletal muscle, heart, and pancreas (12, 13) as well as in male lower urogenital organs (14). *NMDARs* are also expressed in suprabasal keratinocytes, and the activation of NMDA receptors inhibits keratinocyte outgrowth necessary for some epithelialization processes (15). In neurons, *NMDAR* family members exhibit different tissue distributions, expression patterns, and functions. *NMDAR1* is expressed in the vast majority of central neurons throughout all developmental stages in mice, whereas the *NMDAR2* subunits are expressed in distinct spatial and temporal patterns. Prenatal *NMDARs* contain *NMDAR2B* or *NMDAR2D,* whereas *NMDAR2A* and *NMDAR2C* are expressed only after birth (16, 17). In cultured neurons, *NMDAR2A* subunits localize preferentially at synaptic sites and *NMDAR2B* subunits localize extrasynaptically (18). In addition, prenatal lethality was found in *NMDAR2B*$^{-/-}$ (19) and *NMDAR1*$^{-/-}$ (20) mice but not in *NMDAR2A*$^{-/-}$ mice (21).

NMDARs have significant sequence similarity to α-amino-3-hydroxy-5-methyl-4-isoxazolepropionate-type glutamate receptors (*AMPAR*), which mediate fast transmission in excitatory synapses in the central nervous system (22). *AMPARs* are expressed in most glial cells and overexpressed in glioma cells (23), and *AMPAR*-mediated Ca^{2+} permeability plays a crucial role in the tumorigenesis and invasion capacity of glioma (23). Interestingly, aberrant CpG island methylation was reported in the G-protein-coupled metabotropic glutamate receptor 7 of chronic lymphocytic leukemia (24), and the glutamate receptor ionotropic kinate 2 was identified as a candidate

Note: Supplementary data for this article are available at Cancer Research Online (http://cancerres.aacrjournals.org/).

Under a licensing agreement between OncoMethylome Sciences SA and the Johns Hopkins University, Dr. Sidransky is entitled to a share of royalty received by the University on sales of products described in this article. Dr. Sidransky owns OncoMethylome Sciences stock, which is subject to certain restrictions under University policy. Dr. Sidransky is a paid consultant to OncoMethylome Sciences and is a paid member of the company's Scientific Advisory Board. The term of this arrangement is being managed by the Johns Hopkins University in accordance with its conflict of interest policies.

Requests for reprints: David Sidransky, Department of Otolaryngology, Head and Neck Cancer Research Division, Johns Hopkins University School of Medicine, 818 Ross Building, 720 Rutland Avenue, Baltimore, MD 21205-2196. Phone: 410-502-5152; Fax: 410-614-1411; E-mail: dsidrans@jhmi.edu.

doi:10.1158/0008-5472.CAN-05-1608

TSG in acute lymphocytic leukemia (25). However, little is known about the role of *NMDARs* in human cancers.

Esophageal and head and neck squamous cell carcinomas (ESCC and HNSCC, respectively) are the most frequently occurring SCCs. Both heavy smoking and drinking can be crucial risk factors for developing SCCs, and similar genetic changes have been reported in these cancers, such as alterations in the *p53* and *p16* pathways (26, 27). Interestingly, there have been several reports on gene methylation in SCC. *FHIT* was hypermethylated in SCC (14%; ref. 28), and *p16* was also methylated with gene silencing in primary SCC (~15-20%; ref. 29). Recently, *RASSF1* (50%; ref. 30), *trypsinogen-4* (50%; ref. 31), *HLA* class I (40%; ref. 32), and *MGMT* (40%; ref. 33) were all reported to be frequently methylated in primary ESCC.

The combination of pharmacologic unmasking and oligonucleotide microarray techniques enabled us to find novel methylated genes in ESCC cell lines and primary ESCC (34). From these studies, *apolipoprotein D* (80%), *PGP9.5* (60%), and *cyclin A1* (50%) were identified as genes that showed high frequencies of methylation in ESCC. However, the algorithm applied previously did not identify candidate TSGs, which were reactivated by 5-Aza-dC at very low levels. In the current study, we modified the detection method of candidate genes from our previous microarray data to identify more frequently methylated genes with high efficiency in primary cancers. The new method that we developed dramatically improved the rate of identification of novel methylated genes. Among them, *NMDAR2B* was found to have a high frequency of methylation in primary ESCC and strong apoptotic activity in ESCC cell lines.

Materials and Methods

ESCC, normal tissues, and cell lines. Twelve ESCC cell lines, TE1, TE2, TE3, TE4, TE5, KYSE30, KYSE70, KYSE140, KYSE150, KYSE200, KYSE410, and KYSE520, were obtained from the Cell Response Center for Biomedical Research Institute, Department of Aging and Cancer, Tohoku University (Sendai, Japan; TE series) and kindly provided by Dr. Shimada (Department of Surgery, Kyoto University, Kyoto, Japan; KYSE series). Cells were grown in RPMI 1640 supplemented with 10% fetal bovine serum (FBS). Twenty paired ESCC and normal esophagus (patients 1-20) tissues were obtained from the Gastroenterology Division, Department of Medicine, University of Maryland (Baltimore, MD). Forty-four cases of primary ESCC tumors, six paired ESCC, and normal tissue cDNA (patients 72-77) were obtained from patients who underwent surgery at the Medical Institute of Bioregulation Hospital, Kyushu University (Fukuoka, Japan) and the Saitama Cancer Center (Saitama, Japan).

Bisulfite sequencing. Bisulfite-modified genomic DNA was amplified by PCR using 10× buffer [166 mmol/L $(NH_4)_2SO_4$, 670 mmol/L Tris (pH 8.8), 67 mmol/L $MgCl_2$, 0.7% 2-mercaptoethanol, 1% DMSO] and primer sets that were designed to recognize DNA alterations after bisulfite treatment. Primer sequences are shown in Supplementary Table S1. All the PCR products were gel extracted (Qiagen, Valencia, CA) and sequenced with an internal primer (F2) or amplification primer (F1) using the ABI BigDye cycle sequencing kit (Applied Biosystems, Foster City, CA).

Real-time quantitative PCR (Taqman-MSP). For quantitative methylation analysis, PCR primer was designed to hybridize to the region of NMDAR2B that was determined previously to be methylated in ESCC cell lines by sequencing and a fluorescent probe to the amplified region of the DNA. All oligonucleotide primer pairs were purchased from Invitrogen (Carlsbad, CA), and Taqman probe was from VWR (West Chester, PA). The *NMDAR2B* primers had the following sequences: 5′-GAGTATGGTTATTTTTAAAGCG-3′ (*NMDAR2B* TAQF) and 5′-TTAAAACGAATTAATATCTTTTTCG-3′ (*NMDAR2B* TAQR). The NMDAR2B probe was 6FAM 5′-ATTCGCGTGTTTTTCGGAGGGTGA-3′ TAMRA. The *β-actin* primer sequences were 5′-TGGTGATGGAGGAGGTTTAGTAAGT-3′ (*β*-actin TAQF) and 5′-AACCAATAAAACCTACTCCTCCCTTAA-3′ (*β-actin* TAQR). The β-actin probe was 6FAM 5′-ACCACCACCCAACACACAATAACAAACACA-3′ TAMRA. Serial dilutions of human leukocyte genomic DNA, which was methylated *in vitro*, were used to construct a calibration curve, and all reactions were done in duplicate. The methylation ratio was defined as quantity of fluorescence intensity derived from *NMDAR2B* promoter amplification divided by fluorescence intensity from *β-actin* amplification and multiplied by 100 [Taqman methylation value (TaqMeth V)].

5-Aza-dC/TSA treatment and reverse transcription-PCR. Cells were treated with 5 μmol/L 5-Aza-dC (Sigma, St. Louis, MO) every 24 hours for 3 days; TSA (300 nmol/L; Sigma) was added to the medium for the final 24 hours. RNA was extracted using Trizol (Invitrogen) and reverse transcribed with SuperScript II reverse transcriptase (Invitrogen). For amplification of *NMDARs*, touchdown PCR was done as follows: a 5-minute incubation step at 95°C was followed by 2 cycles of 1 minute at 95°C for denaturation, 1 minute at 66°C for annealing, and 1 minute at 72°C for elongation. The annealing temperature was decreased by 2°C, two PCR cycles were run each time until the annealing temperature was 58°C, and PCR was run for 25 cycles and continued for 7 minutes at 72°C for more extension. The primer sequence of *NMDAR2B* was 5′-GCCTGAGCGACAAAAAGTTC-3′ (forward) and 5′-CATCTCCCCATCTCCAAAGA-3′ (reverse). The primer sequence of *NMDAR1A* was 5′-AGACGTGGGTTCGGTATCAG-3′ (forward) and 5′-CTGACCGAGGGATCTGAGAG-3′ (reverse). PCR products were gel extracted and sequenced to verify true expression of the genes. For *β-actin*, regular PCR was done using conditions of 1 minute at 95°C, 1 minute at 58°C, and 1 minute at 72°C for 27 to 30 cycles. *β-actin* primers were 5′-TGGCACCACACCTTCTACAATGAGC-3′ (forward) and 5′-GCACAGCTTCTCCTTAATGTCACGC-3′ (reverse).

Construction of luciferase vectors and reporter assay. Potential *NMDAR2B* promoter regions upstream of the transcription start site (TSS; −1,228 bp and −563 to +28 bp) and in a region downstream of the TSS (+7 to +267 bp) were prepared by PCR using pfx DNA polymerase (Invitrogen). Genomic DNA extracted from the HCT116 human colon cancer cell line was used as template. The forward primers were synthesized corresponding to the upstream sequences of desired promoter regions, and the reverse primers included +28 bp relative to the reported TSS of the human *NMDAR2B* gene. A 3′-flanking *Bgl*II site was added to all reverse primers. The pGL2 promoter control vector (Promega, Madison, WI) was digested with both *Sma*I and *Bgl*II and treated with calf intestinal alkaline phosphatase. The PCR fragments were digested with *Bgl*II and ligated with phosphatase-treated pGL2 vector to generate pGL2-*NMDAR2B* promoter constructs. HCT116 cells were seeded at a density of 4×10^4 per well in a 24-well plate 24 hours before transfection. For each well, plasmid pGL2-*NMDAR2B* promoter constructs (100 ng) were cotransfected with 10 ng control reporter pSV-*Renilla* (Promega) using Fugene 6 (Roche, Basel, Switzerland) in accordance with the manufacturer's instructions. After 48 hours, the luciferase assay was done using a dual luciferase assay kit (Promega). The luciferase activity was normalized by pSV-*Renilla* activity, and pGL2 promoter control vector was used as a negative control. The pGL2-*NMDAR2B*#1 construct that harbors 1,256 kb of PCR fragment were methylated *in vitro* using *Sss*I (CpG) methylase as recommended by the manufacturer's instructions (New England Biolabs, Beverly, MA). After DNA isolation, equal amounts (100 ng) of the methylated or unmethylated luciferase constructs were transfected into HCT116 cells. Each experiment was done twice, each in triplicate.

Transfection and cell treatment. Two separate constructs were used to coexpress the *NMDAR1* and *NMDAR2B* subunits of the *NMDAR*. The rat NMDAR2B expression plasmid (NR2B-pDP3) was kindly provided by Dr. John J. Woodward (Medical University of South Carolina, Charleston, SC), and the rat *NMDAR1A* expression plasmid (*NMDAR1-1a*-pRc/CMV) was kindly provided by Dr. David Lynch (University of Pennsylvania, Philadelphia, PA). After digestion of *NMDAR1-1a*-pRc/CMV with *Hin*dIII and *Not*I, the insert was ligated into pcDNA3.1-Hyg(+) plasmid. ESCC cell lines were transfected using Fugene 6 reagent or calcium phosphate

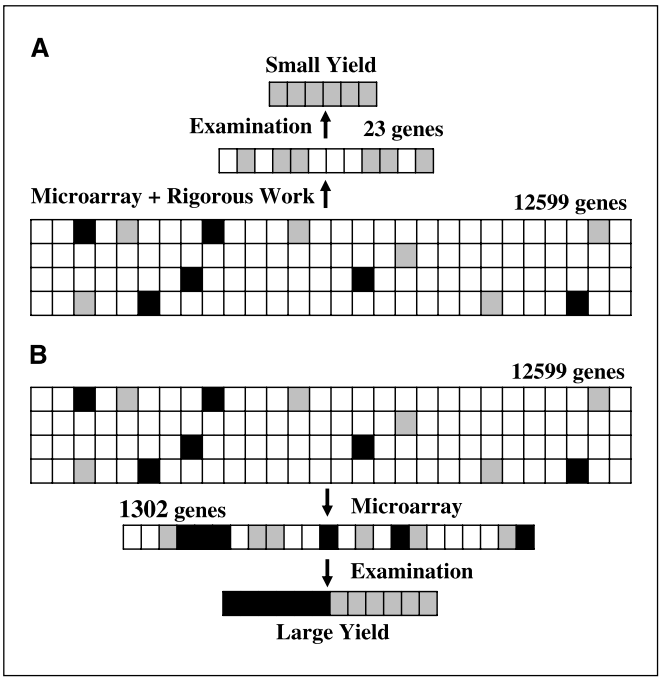

Figure 1. Comparison of results using two different methods to analyze pharmacologic unmasking in ESCC cell lines. *A,* using the previous algorithm to identify methylated genes up-regulated after pharmacologic treatment, rigorous RT-PCR or bisulfite sequencing produced only a relatively small yield of methylated genes. In addition, critical TSGs may have escaped our analysis. *B,* through a simple method using presence or absence of basal expression in untreated cells, about half of the presumed background genes were ruled out without rigorous empirical work resulting in a dramatic improvement in identifying frequently methylated genes. *White,* background genes; *black,* TSGs that evaded the previous algorithm; *gray,* methylated genes.

precipitation in DMEM with 10% FBS. After 24 hours, the medium was changed to MEM with 10% FBS containing no glycine or glutamate (Invitrogen) and incubated for another 24 hours. Then, cells were incubated in serum-free MEM and treated with *NMDAR* agonists and/or inhibitors (Sigma) for 24 hours. NMDA (250 μmol/L) or L-glycine (50 μmol/L)/L-glutamate (200 μmol/L) was treated for *NMDAR* activation, and 10 μmol/L ifenprodil, 10 μmol/L MK-801, 10 μmol/L 6-cyano-7-nitroquinoxaline-2,3-dione (CNQX), or 10 μmol/L BAPTA-AM were used for specific or nonspecific inhibition of *NMDAR*. During transfection, 10 μmol/L MK-801, a general *NMDAR* inhibitor, was added to cells to prevent early activation of *NMDAR* and then removed by washing twice with serum-free MEM before analysis. During agonist-mediated *NMDAR* activation, 50 μmol/L glycine were added to prevent glycine-dependent desensitization of NMDAR.

Cell viability assay. ESCC cells were plated on a 24-well plate at a density of 3×10^4 to 5×10^4 per well and incubated overnight at 37°C. The next day, cells were cotransfected with *NMDAR2B* (0.5 μg) and NMDAR1-1a plasmids (0.5 μg) or with corresponding empty vectors. After treatment with *NMDAR* agonists and antagonists for 24 hours, the tetrazolium-based cell viability [3-(4,5-dimethylthiazol-2-yl)-2,5-diphenyltetrazolium bromide (MTT)] assay was done. The results were expressed as percentage of MTT reduction in samples compared with mock transfectants in the absence of agonists (100%).

DNA fragmentation assay. Cells (1×10^6) in a 10-cm dish were transfected with 5 μg of each plasmid and treated as indicated, and fragmented DNA was isolated using phenol/chloroform extraction. DNA was electrophoresed on a 1.5% agarose gel and stained with ethidium bromide.

Terminal deoxynucleotidyl transferase–mediated nick end labeling assay. Detection of free 3′-OH was done with the DeadEnd fluorometric terminal deoxynucleotidyl transferase–mediated nick end labeling (TUNEL) system (Promega) according to the manufacturer's protocol. Fluorescence was detected with an inverted fluorescence microscope [Nikon (Melville, NY) TE200, HG-100W mercury lamp]. These experiments were done in duplicate and repeated twice.

Caspase activation assay. Caspase-3 and caspase-1 assays were done with Fluorometric CaspACE Assay System (Promega) according to the manufacturer's recommendations. The assay was carried out with 50 μg cellular extracts in triplicate. The fluorescence emitted by the cleaved substrates was read on a Wallac (Wellesley, MA) Victor-1420 microtiter plate fluorometer reader (405 nm).

Flow cytometric analysis. Flow cytometric analysis was done based on the increased ability of apoptotic cells to bind Annexin V-FITC conjugate (PharMingen, San Diego, CA). Cell necrosis was detected by incorporation of 7-amino-actinomycin D dye. Labeled cells were detected by FACScan on a Coulter (Fullerton, CA) Epics XL.

Colony focus assay. Colony focus assays were done as described previously (34) using transfected KYSE140 cells in the presence of G418 (125 μg/mL) for 2 weeks. To confirm the expression of *NMDAR2B,* cells were harvested 48 hours after transfection and reverse transcription-PCR (RT-PCR) was done.

Results

The methylated gene discovery algorithm that was applied in our previous study (34) required excessive experimental effort and time for a relatively small yield through a process of ruling out downstream target genes that were not directly regulated by epigenetic events ("background" genes) using RT-PCR and/or bisulfite sequencing (Fig. 1*A*). Among genes showing high fold increase of expression by pharmacologic unmasking (>3-fold), at most only 10% to 20% were found to be methylated genes, so that 250 to 500 genes were screened to identify 50 novel methylated genes.

To apply a new discovery method for gene methylation, we started with genes that showed increased expression by 5-Aza-dC treatment in all three ESCC cell lines tested (total 2,411 genes), obtained from our previously reported microarray analysis (34). These genes were presumed to exhibit methylation in their promoters and were potentially TSGs. However, these genes were still likely to include many background downstream genes. From

Table 1. Distribution of genes in each experiment

Silenced in*	1 μmol/L 5-Aza-dC	1 μmol/L 5-Aza-dC + 300 nmol/L TSA	5 μmol/L 5-Aza-dC	Genes
3 cell lines (first group)	136 (74)†	115	398	649
2 cell lines (second group)	69 (39)†	100	217	386
1 cell line (third group)	65 (42)†	104	205	374
Total	270 (155)†	319	820	1,302

NOTE: Three independent microarray analyses were done in the previous microarray analysis with cRNA from the cells treated with or without 1 μmol/L 5-Aza-dC, 1 μmol/L 5-Aza-dC plus 300 nmol/L TSA, and 5 μmol/L 5-Aza-dC.

*Cell numbers showing absent basal expression.

†Numbers after ruling out genes without dense CpG sites in the promoter region.

Table 2. Methylation profiles of ESCC cell lines and normal esophageal tissues from both the top group (1-30) and the second priority group (31-45) from Table 1

No.	Accession no.	Gene name	KYSE30	KYSE410	KYSE520	Normal 1	Normal 2	Normal 3	Normal 4
1	M60315	*BMP6*	U	M/U	U	U	U	U	U
2	AB029041	*AZI (KIAA1118)*	M	M	M	M/U	M/U	M/U	M/U
3	M24283	*ICAM-1*	M	M	M	U	U	U	U
4	X07732	*Hepsin*	*	M	*	M/U	M/U	M/U	M/U
5	D64137	*NMDAR2B*	M	M	M	U	U	U	U
6	AB014523	*Unc-51 like*	M	M	M	U	U	*	*
7	X82494	*Fibulin-2*	M	M	M	U	U	U	U
8	J02611	*Apolipoprotein D*	M	M	M	M/U	M/U	M/U	M/U
9	L21715	*Troponin I fast-twitch isoform*	M	M	M	M	M	M	M
10	NM_000170	*Glycine dehydrogenase*	*	M	M	U	U	U	U
11	U27185	*TIG1*	M	M	M	U	U	U	U
12	M55682	*Matrilin-3*	M	M	M	M/U	M/U	M/U	M/U
13	L13203	*Forkhead homologue-3 (HFH-3)*	M	M	M	M/U	M/U	M/U	M/U
14	M84526	*Adipsin*	M	M	M	M/U	M/U	M/U	M/U
15	M65062	*IGFBP5*	U	U	U	U	U	U	U
16	X84740	*DNA ligase III*	U	U	U	U	U	U	U
17	AI094859	*Engrailed-2*	M	M	M	U	U	U	U
18	AB022083	*SOX30*	M	M	M	M	M	*	M
19	U19146	*GAGES*	M	M	M	M	M	M	M
20	AA010777	*Galectin-7*	M/U	*	M/U	M/U	U	*	M/U
21	J04430	*Tartrate-resistant acid phosphatase type 5*	M	M	M	*	M/U	*	MTU
22	U90S42	*SSX5*	M	M	M	M	M	*	M
23	X65293	*Protein kinase C-ϵ*	U	U	M/U	U	U	U	U
24	M69199	*GOS2*	M	M/U	M	*	U	M/U	U
25	M22637	*Lyl-1*	M	M	M	U	U	U	U
26	U02632	*Pendrin*	M	M/U	M/U	M/U	U	M/U	*
27	AB023333	*KIAA1005*	U	U	U	U	U	U	U
28	AB000277	*DAP-1*	M	M	M	M	M	M	M
29	U02687	*Flt-3*	M	M	M	M	M	M	M
30	S76475	*Trk-C*	M	M	M	U	U	U	U
31	U68019	*HMAD3*	U	U	U	*	*	*	*
32	M28439	*Keratin 16*	M	M	M	M/U	M/U	M/U	MTU
33	AB14554	*KIAA0654*	*	U	U	*	*	*	*
34	U33284	*Protein tyrosine kinase PYK2*	U	U	U	*	*	*	*
35	M31682	*Inhibin β-B*	U	U	U	*	*	*	*
36	U29091	*Selenium-binding protein*	M	M	M	M/U	M/U	M/U	M/U
37	J05581	*MUC1*	U	U	U	*	*	*	*
38	M17589	*Tyrosine hydrosylase 4*	M	M	M	M/U	M/U	M/U	M/U
39	U87460	*Endothelin receptor type B-like*	M	M	M	U	U	U	U
40	D26155	*Transcriptional activator hSNF2a (SMARC4)*	U	U	U	U	U	U	U
41	U07804	*DNA topoisomerase I*	U	U	U	U	U	U	U
42	M99439	*Transducin-like enhancer protein (TLE4)*	U	U	U	U	U	U	U
43	AB000714	*Claudin-3*	M/U	M	M	U	U	U	M/U
44	D89337	*MSX-2*	U	*	U	*	U	U	U
45	K15306	*NFH*	M	M	M	U	U	U	U

NOTE: Gene expression was absent in three ESCC cell lines (first group 1-30) and in two of three cell lines (second group 31-45) by microarray results. Abbreviations: M, harbor methylated alleles alone; M/U, harbor both methylated and unmethylated alleles; U, harbor unmethylated alleles alone; *, not assessed.

previous empirical studies, we observed that there was a striking difference in expression between methylated and unmethylated genes (34). Genes that exhibited promoter methylation showed no basal expression in all cell lines tested ($P < 0.00001$), suggesting that genes with basal expression in cancer cell lines were unlikely to harbor promoter methylation. Based on these observations, we ruled out genes that were expressed in any of the three cancer cell lines in the absence of any treatment. This process allowed us to easily remove about half of the presumed background from our candidate gene list (1,302 genes remained; Fig. 1*B*).

The 1,302 genes were derived from three different pharmacologic treatments: 270 genes from 1 μmol/L 5-Aza-dC treatment, 319 genes from 1 μmol/L 5-Aza-dC plus 300 nmol/L TSA treatment, and 820 genes from 5 μmol/L 5-Aza-dC treatment (Table 1).

Overlapping genes among the individual experiments were relatively few (data not shown). We chose to focus on reexpressed genes after 1 μmol/L 5-Aza-dC treatment (270 genes) for our pilot study. Although fold increase under this latter treatment was smaller, it was most likely to result in the least number of background genes compared with more aggressive treatments.

About 40% (115) of the genes were ruled out because they did not harbor CpG sites in their promoter regions (155 genes remained). Among the remaining 155 genes, 74 (first group) were silenced in all three cell lines examined by microarray, the second group (39 genes) showed absent in expression in two of three cells lines, and the third group (42 genes) in only one cell line. We reasoned that genes frequently methylated in primary ESCC would also be frequently methylated in ESCC cell lines. Thus, we focused on the first and second groups of genes.

We randomly selected 30 and 15 genes from the first and the second groups, respectively, and examined their gene promoters for methylation in three ESCC cell lines by bisulfite sequencing (Table 2). Consequently, 33 of 45 novel methylated genes were identified. Remarkably, promoter methylation in ESCC cell lines was correctly predicted by this approach in 90% (27 of 30) among the first group of genes and 40% (6 of 15) among the second group of genes.

We also examined promoter methylation status in four normal esophageal mucosa samples to rule out genes methylated in normal tissues. As a result, among the 33 methylated genes examined in the pilot study, only 11 genes showed methylation in all three ESCC cell lines but not in the four normal esophageal tissues (cancer-specific methylation; 33%; Table 2). Twenty genes were methylated in normal tissues, and the remaining two genes (*BMP6* and *PKC-ϵ*) were infrequently or weakly methylated in the ESCC cell lines. Among the 20 genes methylated in normal tissues, 14 genes harbored both methylated and unmethylated alleles (72.7%) and the remaining 6 genes, which included tumor antigens, such as *GAGE5* and *SSX5*, only harbored methylated alleles (27.3%).

Eleven genes that showed cancer-specific methylation (3 of 3 in ESCC cell lines; 0 of 4 in normal tissues) were examined in primary ESCC by bisulfite sequencing (Fig. 2*A*). Five genes showed no methylation in primary ESCC (*ICAM-1, Fibulin-2, Unc-51, Lyl-1,* and *endothelin receptor type B-like*), indicating that methylation of these genes may have occurred during cancer cell line propagation. *Glycine dehydrogenase* [3 of 10 (30%) cases], *Trk-C* [2 of 15 (12.5%)], and *TIG1* [1 of 8 (12.5%)] were methylated with relatively low frequencies. Neurofilament heavy chain (*NFH*) and

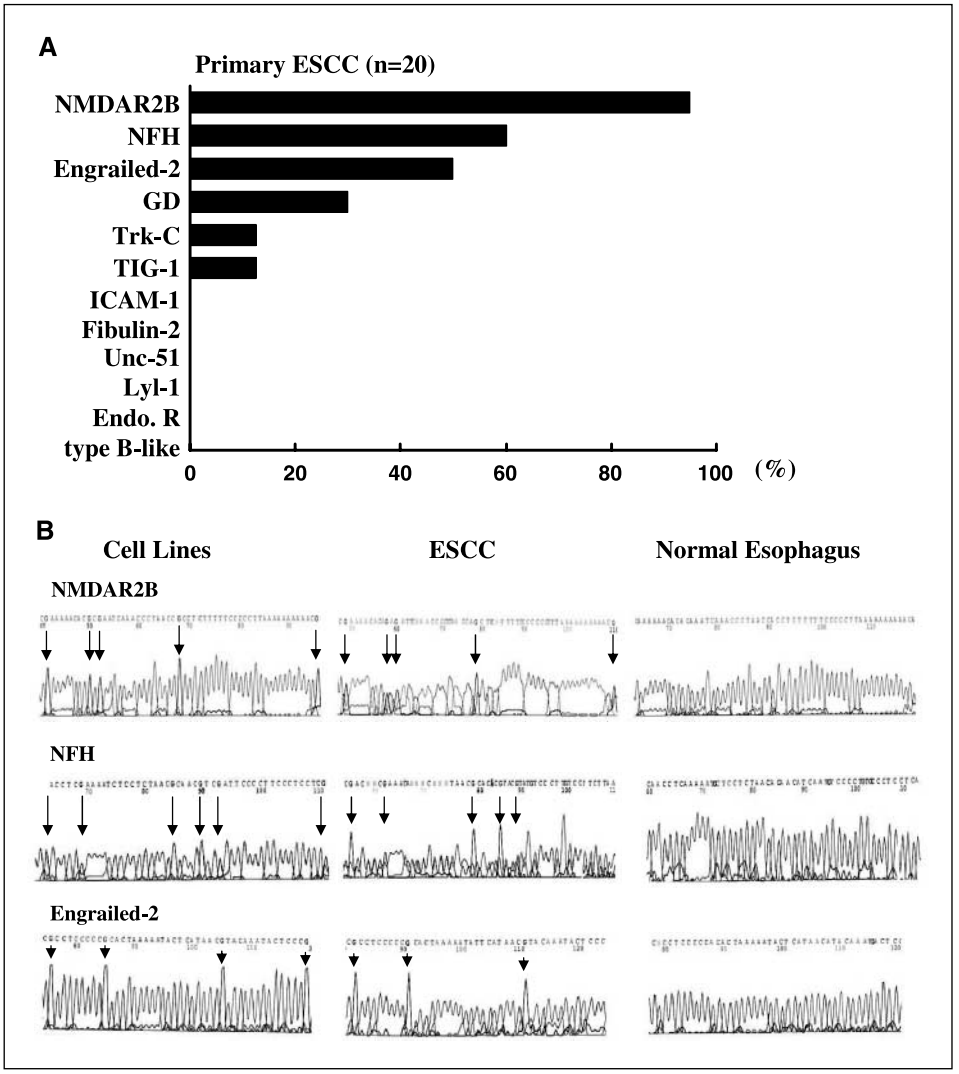

Figure 2. Promoter methylation of representative candidate genes. *A,* methylation frequencies of 11 candidate genes in 20 ESCC tissues that were frequently methylated in three ESCC cell lines (KYSE30, KYSE410, and KYSE520) but not in four normal tissues. The *NMDAR2B* promoter was analyzed by direct sequencing of bisulfite-treated genomic DNA. *Endo. R type B-like, endothelin receptor type B-like;* %, methylation frequency in primary ESCCs. *B,* representative sequencing results of the *NMDAR2B, NFH,* and *engrailed-2* gene promoters in ESCC cell lines (KYSE30, KYSE410, or KYSE520) and primary ESCCs compared with normal esophagus. Normal tissues were taken from normal-appearing distal mucosa in patients with ESCCs. *Arrows,* all guanines present after sequencing that are complementary to methyl cytosines on the opposite DNA strand.

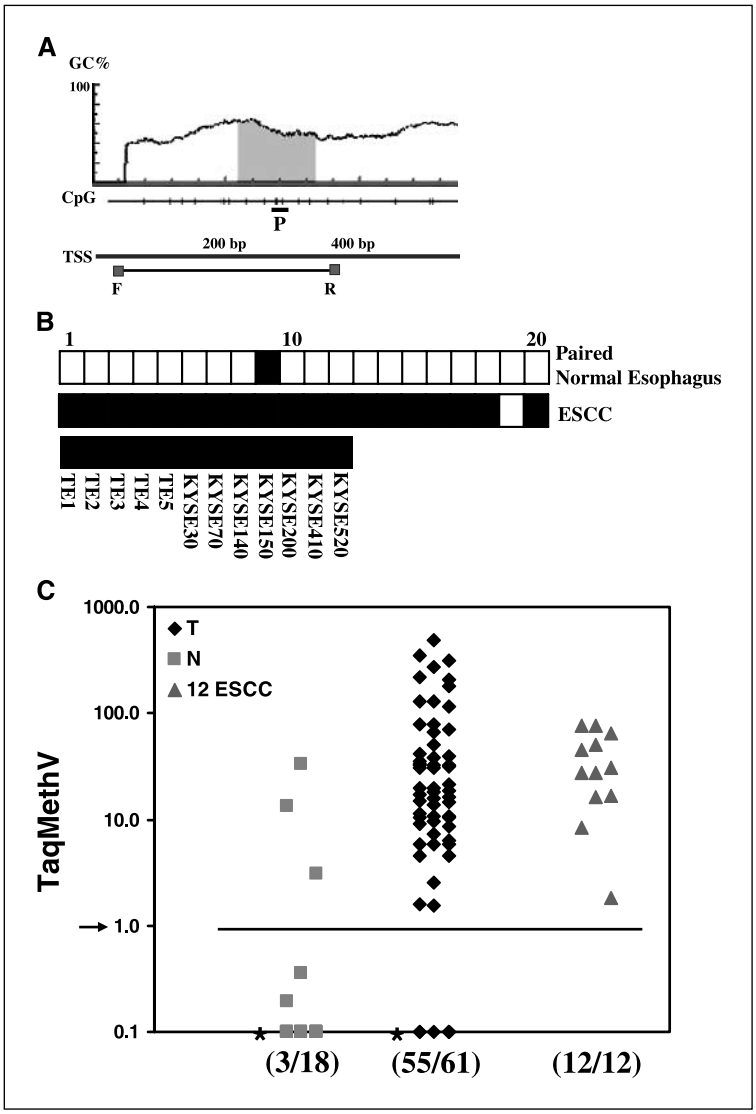

Figure 3. Methylation and expression of *NMDAR2B* in primary tumors. *A,* position of CpG islands (*blue*) in the 600-bp region upstream of the TSS in the *NMDAR2B* promoter. *F* and *R,* primers for bisulfate DNA amplification; *P,* probe used for Taqman-MSP analysis of *NMDAR2B*. *B,* methylation of the *NMDAR2B* promoter in normal esophageal mucosa (*top*), corresponding primary tumors (*middle*), and 12 ESCC cell lines (*bottom*). In 12 ESCC cell lines, *NMDAR2B* was methylated 100%. *Black box,* methylation; *white box,* no methylation. *C,* scatter plot of quantitative analysis of *NMDAR2B* promoter methylation. Taqman-MSP was done to analyze the *NMDAR2B* promoter methylation in 61 ESCC and 18 normal tissues. Cases in ESCCs (55 of 61) and all ESCC cell lines tested were detected as methylated by Taqman-MSP, and 15 of 18 cases in normal esophageal tissues were below the cutoff. *Arrow* and *horizontal bar,* cutoff value as 1. *Asterisks,* samples with a ratio equal to zero could not be plotted correctly on a log scale. TaqMeth V is described in Materials and Methods.

engrailed-2 were frequently methylated [12 of 20 (60%) and 9 of 18 (50%), respectively] in ESCC but not as frequently in corresponding matched normal-appearing tissues at some distance from the tumor itself [0 of 18 (0%) and 3 of 19 (15.8%), respectively], indicating that they were methylated in a cancer-specific manner. Among the 11 cancer specifically methylated genes, *NMDAR2B* showed the highest frequency of methylation in primary ESCC [19 of 20 cases (95%)] and a very low frequency in matched normal-appearing esophageal mucosa [1 of 20 cases (5%); Figs. 2*B* and 3*B*].

To study *NMDAR2B* promoter methylation, we analyzed the region directly upstream of the TSS that harbors CpG islands (<600 bp) by bisulfite sequencing (Fig. 3*A*). All 12 ESCC cell lines examined showed methylation in the region and, significantly, exhibited silencing of *NMDAR2B* mRNA expression (Fig. 4*A, left*), suggesting that mRNA expression of *NMDAR2B* was regulated by promoter hypermethylation. Taqman-MSP analysis with a probe targeted to the CpG island of *NMDAR2B* was done in 18 normal esophageal mucosa and 61 primary ESCC samples that included 17 primary ESCC tissues analyzed previously by bisulfite sequencing. In some normal-appearing tissues, very low levels of promoter methylation were detected by Taqman-MSP, which has a higher sensitivity than bisulfite sequencing. The TaqMeth V detected in primary ESCCs were significantly higher than in normal tissues (Fig. 3*C*). Methylation of *NMDAR2B* was found in all ESCC cell lines (12 of 12 cells; cutoff 1) and in primary ESCC [55 of 61 cases (90.16%)]. The three paired normal tissues with higher levels likely contained infiltrating neoplastic clones from the primary cancers.

NMDAR2B expression was robustly reactivated by the demethylating agent 5-Aza-dC in 5 ESCC cell lines (KYSE30, KYSE140, KYSE200, KYSE410, and KYSE520; Fig. 4*B*). The reactivation was stronger in KYSE30, KYSE410, and KYSE520 when both 5-Aza-dC and 300 nmol/L TSA were used in combination. Among the six ESCC primary tumor and normal pairs, mRNA expression of *NMDAR2B* was silenced (patients 73 and 76) or reduced (patients 74 and 77) in primary ESCC compared with corresponding normal tissues (Fig. 4*A, right*). Promoter methylation status of these tissues was unavailable due to insufficient quantities of DNA. Although *NMDAR1A* expression was also silenced in 9 of 12 ESCC cell lines (Fig. 4*C*), the *NMDAR1* promoter was methylated in all 12 ESCC cells tested (data not shown), indicating that the expression of

NMDAR1A was not completely dependent on the specific methylation pattern in cell lines.

To examine the effect of *NMDAR2B* promoter methylation on gene expression, we made three reporter constructs containing different portions of the unmethylated *NMDAR2B* promoter sequences (position −1,228 to +267 bp) relative to the TSS (Fig. 4*D*). Construct pGL2-*NMDAR2B#2* (−563 to +28 bp) had the highest promoter activity of all the constructs as shown by luciferase assay in HCT116 cells (Fig. 4*D*). The pGL2-*NMDAR2B#1* construct (−1228 to +28 bp) had similar activity with pGL2-*NMDAR2B#2,* whereas construct pGL2-*NMDAR2B#3* (+7 to +267 bp) had minimal promoter activity. To investigate the role of DNA methylation in regulation of *NMDAR2B* expression, we treated the pGL2-*NMDAR2B#1* construct with *Sss*I methylase (Fig. 4*E*). Promoter activity of the methylated pGL2-*NMDAR2B#1* construct was ~18 times lower than that of the unmethylated pGL2-*NMDAR2B#1* construct.

It is known that primary neurons grown in culture die when exposed to glutamate because of excess excitation through glutamate receptors (35). Cell death can be prevented by blocking *NMDARs* or by removing calcium from the cell culture medium, suggesting that *NMDAR*-mediated Ca^{2+} permeability may play a critical role in the process of neuronal apoptosis (36). Thus, having determined that *NMDAR2B* is frequently methylated, we examined its potential tumor suppressor function in ESCC cell lines.

NMDAR1-1a and *NMDAR2B,* which together compose functional *NMDARs,* were both transfected into 12 ESCC cell lines with or without agonists (NMDA or Gly/Glu), and MTT assays were done to evaluate cell viability. ESCC cell lines (10 of 12) exhibited varying degrees of cell death in the presence of *NMDAR1-1a* and *NMDAR2B* when treated with NMDA or Gly/Glu (Supplementary Fig. S1A). Because KYSE140 did not express either *NMDAR1A* or *NMDAR2B* mRNA (Fig. 4*A* and *C*) and was most sensitive to NMDAR-induced cell death in the presence of NMDA or Gly/Glu, we analyzed this cell line further.

In nontransfected KYSE140 cells, Gly/Glu did not have any toxic effect (Supplementary Fig. S1B). However, transfection of *NMDAR1-1a* and *NMDAR2B* dramatically decreased KYSE140 cell viability in the presence of Gly/Glu (Fig. 5*A*) or NMDA (Supplementary Fig. S1C). The *NMDAR2B*-specific inhibitor ifenprodil partially prevented *NMDAR*-induced cell death and, to a lesser extent, the noncompetitive *NMDAR* antagonist MK-801. A nonspecific *NMDAR* antagonist, CNQX, as well as the intracellular calcium chelator, BAPTA-AM, had little protective effect.

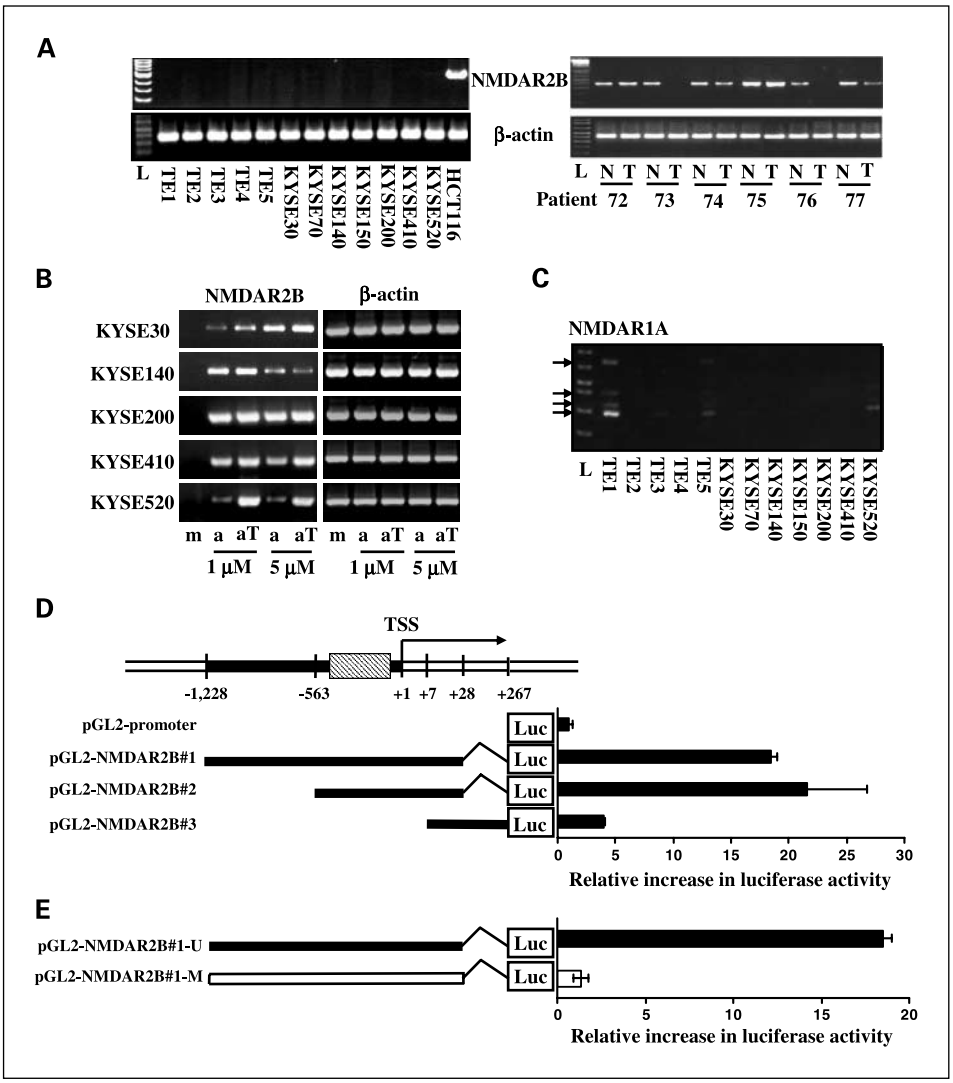

Figure 4. Promoter hypermethylation silences expression of *NMDAR2B*. *A, left, NMDAR2B* was completely silenced in ESCC cell lines; *right,* expression of *NMDAR2B* in ESCC tissues as detected by RT-PCR. *NMDAR2B* in tumors (*T*) showed reduction in expression compared with normal mucosa (*N*). cDNA from a colorectal cell line, HCT116, was used as a positive control for RT-PCR because it expressed *NMDAR2B*. *β-Actin* was used as a loading control. *L,* 1 kb plus DNA ladder. *B,* reactivation of silenced *NMDAR2B* by 5-Aza-dC (*a*) and/or TSA (*T*) treatments. *m,* no treatment. *C,* 9 of 12 ESCC cell lines exhibited silencing of *NMDAR1A*. *Arrows,* splice variants of *NMDAR1A*, determined by sequencing of RT-PCR products after gel extraction. *D,* analysis of *NMDAR2B* promoter activity by luciferase reporter assay in HCT116 cells. Different portions of the unmethylated *NMDAR2B* promoter were tested for luciferase activity. Relative luciferase activity for each construct relative to the activity of the pGL2 promoter control vector. *Shaded box,* between −563 and +1 bp is the region in which *NMDAR2B* promoter methylation was analyzed. *E,* promoter methylation of the *NMDAR2B* 5′ region inhibits luciferase activity. *M, open rectangle,* pGL2-*NMDAR2B1* construct was treated with *Sss*I methylase. *U, filled rectangle,* luciferase activity was assayed after transfection of HCT116 cells and is reported relative to the unmethylated control construct.

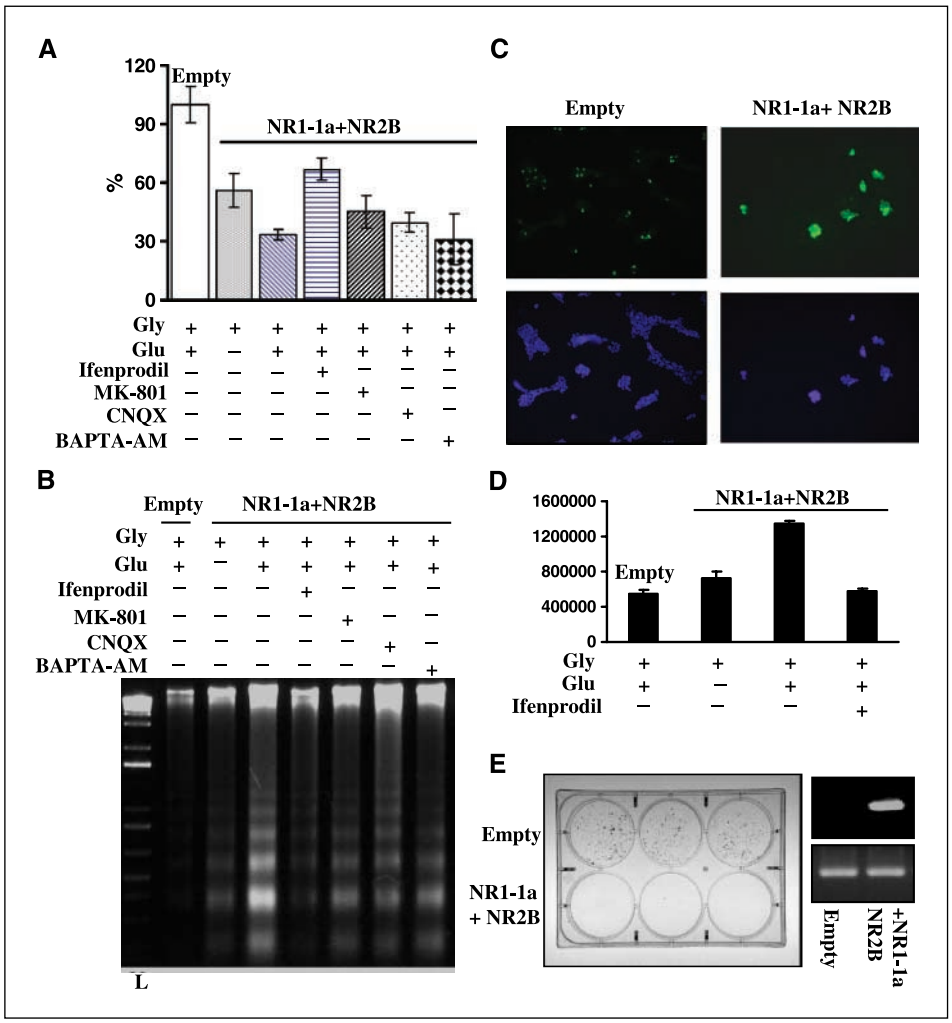

Figure 5. *NMDAR2B*-induced apoptosis in KYSE140 ESCC cell line. *A,* cell viability after transfection of both rat *NMDAR1-1a* and *NMDAR2B* into KYSE140 cells with or without agonists (Gly/Glu; 50 μmol/L/200 μmol/L). Ifenprodil (10 μmol/L), specific inhibitor of *NMDAR2B*; MK-801 (10 μmol/L), nonspecific inhibitor of *NMDAR*; CNQX (10 μmol/L), *AMPA* receptor antagonist; and BAPTA-AM (10 μmol/L), calcium chelator. %, cell viability compared with empty vector-transfected cells in the presence of agonists (100%). *Columns,* mean of triplicate experiments; *bars,* SD. *Empty,* mock transfection. *B,* DNA fragmentation assay was done in KYSE140 cells after transfection with *NMDARs*. *L,* 1 kb plus DNA ladder. *C, top,* cells were transfected with *NMDARs*, and a TUNEL assay was done; *bottom,* all nuclei were stained with 4′,6-diamidino-2-phenylindole. DNase I (10 units) was used as a positive control for the induction of apoptosis. Magnification, ×100. *D,* caspase-3 activation assay. Relative caspase-3 activity was measured by subtracting background (*blank*) and fluorescence units (*Y axis value*) in the presence of the specific caspase-3 inhibitor Ac-DEDV-CHO. *E, left,* colony focus assays were done after transfection of KYSE140 cells in triplicate. Cells were incubated in the presence of G418 (125 μg/mL) for 2 weeks and stained with 0.4% crystal violet solution (methanol/acetic acid; 3:1). *Right,* to confirm the expression of *NMDAR2B*, cells were harvested 48 hours after transfection and RT-PCR was done.

In addition, morphologic alterations, including rounding, appearance of apoptotic bodies, and nuclear shrinkage, were seen in KYSE140 cells transfected with *NMDAR1-1a* and *NMDAR2B*, suggesting that cells were in the process of apoptosis (data not shown). To determine if cells experiencing *NMDAR*-induced death were undergoing apoptosis, DNA fragmentation assays were done. As shown in Fig. 5*B*, the results were consistent with that of MTT analysis above. Internucleosomal cleavage (DNA ladder) induced by *NMDAR2B* activation in the presence of Gly/Glu was inhibited specifically by ifenprodil. Moreover, the TUNEL assay, which detects DNA strand breaks by labeling free 3′-OH termini, showed that *NMDAR*-transfected cells were undergoing early stages of apoptosis (Fig. 5*C*). The specific protective role of ifenprodil in *NMDAR2B*-activated apoptosis was also clearly seen in the TUNEL assay (Supplementary Fig. S3), whereas the other NMDAR antagonist and BAPTA-AM did not have any effect. Data from flow cytometric analysis of Annexin V staining (Supplementary Fig. S1D) and caspase-3 activity (Fig. 5*D*) also indicated that NMDAR2B activation was able to induce apoptosis in KYSE140 cells. To assess long-term growth, colony focus assays were done after treatment of transfected cells with the plasmid selection marker, G418 (Fig. 5*E*). *NMDAR2B* showed potent tumor-suppressive activity by markedly reducing the colony-forming ability of the cells. A similar effect was observed after cotransfection of *NMDAR2B* and *NMDAR1-1a*-pcDNA3.1-Hyg after selection with hygromycin and G418 together (data not shown). In addition, we observed similar results in another ESCC cell line, KYSE30 (Supplementary Figs. S2 and S3).

Discussion

Malignancies of the upper gastrointestinal tract, including ESCC, gastric adenocarcinoma, and adenocarcinoma of the gastric cardia, have distinct clinical and molecular characteristics. These cancers are often diagnosed at an advanced stage and are generally associated with a poor patient prognosis. The key similarities and differences between ESCC and esophageal adenocarcinoma have been compared from a molecular biology standpoint (37). However, the underlying mechanisms that determine the biological and molecular behaviors of ESCC have not been fully elucidated because most current studies focus on esophageal adenocarcinoma. Thus, finding molecular therapeutic targets for ESCC treatment is a promising avenue of research that may help improve the survival of patients with this type of cancer.

Genes methylated in primary cancers at high frequency may serve as biomarkers for the early detection of cancers (38–44). Genes that exhibit cancer-specific methylation at a high frequency in primary tumors may harbor tumor suppressive activity (45–49). The new analysis we developed in this study allowed us to identify

methylated genes from microarray data with high accuracy (90% in the first group; Table 1). Using software predictions, the highest reported accuracy was 82% retrospectively, with which a computer algorithm predicted methylation-prone genes in cell lines (50). Our detection method did not rely on specific software; we simply ruled out presumed background genes and prioritized the candidates according to the microarray data. If we assume a methylation frequency of 40% in the second group and ~20% in the third group, the average frequency of methylated genes among the first three groups of candidates is ~50%. Thus, theoretically applying this simple method to all candidate genes (1,302) should yield ~20 novel methylated genes ($1{,}302 \times 0.5 \times 0.03 \cong 20$).

Our results revealed gene methylation discrepancies between cancer cell lines and primary tumors (Fig. 2*B*). From our analysis, 33 genes were methylated in all three ESCC cell lines tested, but only 3 genes were methylated in primary ESCCs with >50% frequency [3 of 33 (9.1%)]. In addition, promoter hypermethylation was often present in paired normal esophagus tissues [20 of 33 (60.6%)]. Among 11 genes that were methylated in three ESCC cell lines but not in four normal esophagus samples (Table 1), only 3 genes were methylated in primary ESCCs without any evidence of even low level of methylation in paired normal tissues [i.e., absolutely cancer-specific methylation; 3 of 11 (27.3%)].

Gene expression of *NMDAR2B* displayed an inverse correlation with gene methylation (Figs. 3 and 4). Reactivation of its expression by demethylation agents and no detection of allelic loss at chromosomal region *12p12* (data not shown) suggest that *NMDAR2B* inactivation in human cancers occurs mainly through epigenetic events.

NMDAR signaling and the mechanism of *NMDAR*-involved apoptosis have been studied intensively in neurons (9, 36), and the functional exploration of *NMDAR2B* in our study suggests that it may function as a TSG in human tumors (Fig. 5). *NMDAR*-mediated apoptosis was clearly shown in human ESCC cell lines and was blocked by the specific *NMDAR2B* inhibitor, ifenprodil. Surprisingly, BAPTA-AM, the calcium chelator, was unable to protect cells against *NMDAR2B*-induced apoptosis. These results stand in contrast to previous work done in neurons (9, 36), indicating that the functional reconstitution of *NMDAR*-induced apoptosis in cancer epithelial cell lines occurs through a mechanism independent of Ca^{2+} permeability.

Nitric oxide (NO) produced by neuronal NO synthase (*nNOS*) also plays an important role in *NMDAR*-dependent neurotoxicity in neurons (9). Physical coupling of functional *NMDARs* and *nNOS* activation is mediated by an intermediary adaptor protein, PSD95 (*Dlg-4*; ref. 51). The PDZ domain of the major postsynaptic density protein (*PSD95*) specifically binds to the COOH terminus of the *NMDAR2B* subunits of the *NMDARs* (52). *PSD95* is expressed in epithelial cells (53) and has homology with *Drosophila* large discs (*Dlg*), which are TSGs (54). It is intriguing that recessive lethal mutations in *Dlg* interfere with the formation of tight junctions between epithelial cells, which can cause neoplastic overgrowth of imaginal discs (55, 56). In addition, the tumor suppressor *PTEN* physically associates with the *NMDAR1* and *NMDAR2B* subunits of *NMDARs* in rat hippocampus (57) and the colorectal tumor suppressor *APC* is present in the NMDA receptor-PSD95 complex in the brain (58). Thus, it is possible that *PSD95, PTEN,* and/or *APC* might be involved in *NMDAR2B*-induced apoptosis in human cancers. Future work will focus on the investigation of specific pathways in *NMDAR2B*-induced apoptosis.

In summary, our simple, more focused analysis was efficient in identifying a potential candidate TSG, *NMDAR2B*. To our knowledge, this is the first report of promoter methylation and apoptotic activity of *NMDAR2B* in human ESCCs. In addition to providing a very high frequency biomarker in ESCC, the tumor suppressive aspects of *NMDAR2B* open new avenues of research in cancer biology.

Acknowledgments

Received 5/17/2005; revised 12/23/2005; accepted 1/23/2006.

Grant support: NCI grant P50-CA 96784 and a collaborative research agreement with OncoMethylome Science.

The costs of publication of this article were defrayed in part by the payment of page charges. This article must therefore be hereby marked *advertisement* in accordance with 18 U.S.C. Section 1734 solely to indicate this fact.

References

1. Jones P, Veenstra G, Wade P, et al. Methylated DNA and MeCP2 recruit histone deacetylase to repress transcription. Nat Genet 1998;19:187–91.
2. Nan X, Ng H, Jonson C, et al. Transcriptional repression by the methyl-CpG-binding protein MeCP2 involves a histone deacetylase complex. Nature (Lond) 1998;393:386–9.
3. Herman J, Baylin S. Gene silencing in cancer in association with promoter hypermethylation. N Eng J Med 2003;349:2042–54.
4. Feinberg A, Vogelstein B. Hypomethylation of ras oncogenes in primary human cancers. Biochem Biophys Res Commun 1983;111:47–54.
5. Feinberg A, Vogelstein B. Hypomethylation distinguishes genes of some human cancers from their normal counterparts. Nature (Lond) 1983;301:89–92.
6. Cameron E, Bachman K, Myohanen S, Herman J, Baylin S. Synergy of demethylation and histone deacetylase inhibition in the reexpression of genes silenced in cancer. Nat Genet 1999;21:103–7.
7. Presant C, Valeriote F, Vietti T. Biological characterization of a prolonged antileukemic effect of 5-azacytidine. Cancer Res 1977;37:376–81.
8. Belinsky S, Klinge D, Stidley C, et al. Inhibition of DNA methylation and histone deacetylation prevents murine lung cancer. Cancer Res 2003;64:7089–93.
9. Boehning D, Snyder S. Novel neural modulators. Annu Rev Neurosci 2003;26:105–31.
10. Moriyoshi K, Masu M, Ishii T, Shigemoto R, Mizuno N, Nakanishi S. Molecular cloning and characterization of the rat NMDA receptor. Nature (Lond) 1991;354:31–7.
11. Nakazawa K, McHugh T, Wilson M, Tonegawa S. NMDA receptors, place cells, and hippocampal spatial memory. Nat Rev Neurosci 2004;5:361–72.
12. Grozdanovic Z, Gossrau R. Colocalization of nitric oxide synthase I (NOS I) and NMDA receptor subunit 1 (NMDAR-1) at the neuromuscular junction in rat and mouse skeletal muscle. Cell Tissue Res 1998;291:57–63.
13. Lin YJ, Bovetto S, Carver JM, Giordano T. Cloning of the cDNA for the human NMDA receptor NR2C subunit and its expression in the central nervous system and periphery. Brain Res Mol Brain Res 1996;43:57–64.
14. Gonzalez-Cadavid NF, Ryndin I, Vernet D, Magee TR, Rajfer J. Presence of NMDA receptor subunits in the male lower urogenital tract. J Androl 2000;21:566–78.
15. Nahm WK, Philpot BD, Adams MM, et al. Significance of *N*-methyl-D-aspartate (NMDA) receptor-mediated signaling in human keratinocytes. J Cell Physiol 2004;200:309–17.
16. Monyer H, Burnashev N, Laurie DJ, Sakmann B, Seeburg PH. Developmental and regional expression in the rat brain and functional properties of four NMDA receptors. Neuron 1994;12:529–40.
17. Akazawa C, Shigemoto R, Bessho Y, Nakanishi S, Mizuno N. Differential expression of five *N*-methyl-D-aspartate receptor subunit mRNAs in the cerebellum of developing and adult rats. J Comp Neurol 1994;347:150–60.
18. Li JH, Wang YH, Wolfe BB, et al. The incorporation of NMDA receptors with a distinct subunit composition at nascent hippocampal synapses *in vitro*. J Neurosci 1999;19:4180–8.
19. Kutsuwada T, Sakimura K, Manabe T, et al. Impairment of suckling response, trigeminal neuronal pattern formation, and hippocampal LTD in NMDA receptor ε2 subunit mutant mice. Neuron 1996;16:333–44.
20. Forrest D, Yuzaki M, Soares HD, et al. Targeted disruption of NMDA receptor 1 gene abolishes NMDA response and results in neonatal death. Neuron 1994;13:325–38.
21. Sakimura K, Kutsuwada T, Ito I, et al. Reduced hippocampal LTP and spatial learning in mice lacking NMDA receptor ε1 subunit. Nature 1995;373:151–5.
22. Lamprecht R, LeDoux J. Structural plasticity and memory. Nat Rev Neurosci 2004;5:45–54.
23. Ishiuchi S, Tsuzuki K, Yoshida Y, et al. Blockage of Ca^{2+}-permeable AMPA receptors suppresses migration and induces apoptosis in human glioblastoma cells. Nat Med 2002;8:971–8.
24. Rush LJ, Raval A, Funchain P, et al. Epigenetic profiling in chronic lymphocytic leukemia reveals novel methylation targets. Cancer Res 2004;64:2424–33.

25. Sinclair PB, Sorour A, Martineau M, et al. A fluorescence *in situ* hybridization map of 6q deletions in acute lymphocytic leukemia: identification and analysis of a candidate tumor suppressor gene. Cancer Res 2004;64:4089–98.

26. Mandard A, Hainaut P, Hollstein M. Genetic steps in the development of squamous cell carcinoma of the esophagus. Mutat Res 2000;462:335–42.

27. Forastiere A, Koch W, Trotti A, Sidransky D. Head and neck cancer. N Engl J Med 2001;345:1890–900.

28. Tanaka H, Shimada Y, Harada H, et al. Methylation of the 5′ CpG island of the FHIT gene is closely associated with transcriptional inactivation in esophageal squamous cell carcinomas. Cancer Res 1998;58:3429–34.

29. Merlo A, Herman J, Mao L, et al. 5′ CpG island methylation is associated with transcriptional silencing of the tumour suppressor p16/CDKN2/MTS1 in human cancers. Nat Med 1995;1:686–92.

30. Kuroki T, Trapasso F, Yendamuri S, et al. Allele loss and promoter hypermethylation of VHL, RAR-b, RASSF1A, FHIT tumor suppressor genes on chromosome 3p in esophageal squamous cell carcinoma. Cancer Res 2003;64:3724–8.

31. Yamashita K, Mimori K, Inoue H, Mori M, Sidransky D. A tumor suppressive role for trypsin in human cancer progression. Cancer Res 2003;63:6575–8.

32. Nie Y, Yang G, Song Y, et al. DNA hypermethylation is a mechanism for loss of expression of the HLA class I genes in human esophageal squamous cell carcinomas. Carcinogenesis 2001;22:1615–23.

33. Zhang L, Lu W, Miao X, Xing D, Tan W, Lin D. Inactivation of DNA repair gene O^6-methylguanine-DNA methyltransferase by promoter hypermethylation and its relation to p53 mutations in esophageal squamous cell carcinoma. Carcinogenesis 2003;24:1039–44.

34. Yamashita K, Upadhay S, Osada M, et al. Pharmacological unmasking of epigenetically silenced tumor suppressor genes in esophageal squamous cell carcinoma. Cancer Cell 2002;2:485–500.

35. Hardingham G, Fukunaga Y, Bading H. Extrasynaptic NMDARs oppose synaptic NMDARs by triggering CREB shut-off and cell death pathway. Nat Neurosci 2002;5: 405–14.

36. Anegawa N, Guttmann R, Grand E, Anand R, Lindstrom J, Lynch D. *N*-methyl-D-aspartate receptor mediated toxicity in nonneuronal cell lines: characterization using fluorescent measures of cell viability and reactive oxygen species production. Mol Brain Res 2000;77:163–75.

37. Lin J, Beerm DG. Molecular biology of upper gastrointestinal malignancies. Semin Oncol 2004;31: 476–86.

38. Esteller M, Sanchez-Cespedes M, Rosell R, Sidransky D, Baylin SB, Herman JG. Detection of aberrant promoter hypermethylation of tumor suppressor genes in serum DNA from non-small cell lung cancer patients. Cancer Res 1999;59:67–70.

39. Kawakami K, Brabender J, Lord RV, et al. Hypermethylated APC DNA in plasma and prognosis of patients with esophageal adenocarcinoma. J Natl Cancer Inst 2000;92:1805–11.

40. Sanchez-Cespedes M, Esteller M, Wu L, et al. Gene promoter hypermethylation in tumors and serum of head and neck cancer patients. Cancer Res 2000;60: 892–5.

41. Jeronimo C, Usadel H, Henrique R, et al. Quantitation of GSTP1 methylation in nonneoplastic prostatic tissue and organ-confined prostate adenocarcinoma. J Natl Cancer Inst 2001;93:1747–52.

42. Usadel H, Brabender J, Danenberg KD, et al. Quantitative adenomatous polyposis coli promoter methylation analysis in tumor tissue, serum, and plasma DNA of patients with lung cancer. Cancer Res 2002;62: 371–5.

43. Harden S, Sanderson H, Goodman S, et al. Quantitative GSTP1 methylation and the detection of prostate adenocarcinoma in sextant biopsies. J Natl Cancer Inst 2003;95:1634–7.

44. Hoque M, Begum S, Topalogu O, et al. Quantitative detection of promoter hypermethylation of multiple genes in the tumor, urine, and serum DNA of patients with renal cancer. Cancer Res 2004;64:5511–7.

45. Li Q-L, Ito K, Sakakura CF, et al. Causal relationship between the loss of RUNX3 expression and gastric cancer. Cell 2002;109:113–24.

46. Yoshikawa H, Matsubara K, Qian GS, et al. SOCS-1, a negative regulator of the JAK/STAT pathway, is silenced by methylation in human hepatocellular carcinoma and shows growth-suppression activity. Nat Genet 2001;28: 29–35.

47. Dammann R, Li C, Yoon JH, Chin PL, Bates S, Pfeifer GP. Epigenetic inactivation of a RAS association domain family protein from lung tumor suppressor locus 3p21.3. Nat Genet 2000;25:315–19.

48. Suzuki H, Gabrielson E, Chen W, et al. A genomic screen for genes up-regulated by demethylation and histone deacetylase inhibition in human colorectal cancer. Nat Genet 2002;31:141–9.

49. Suzuki H, Watkins D, Jair K, Schuebel K, et al. Epigenetic inactivation of SFRP genes allows constitutive WNT signaling in colorectal cancer. Nat Genet 2004;36:417–22.

50. Feltus F, Lee E, Castello J, Plass C, Vertino P. Predicting aberrant CpG island methylation. Proc Natl Acad Sci U S A 2003;100:12253–8.

51. Kornau H, Schenker L, Kenned M, Seeburg P. Domain interaction between NMDA receptor subunits and the postsynaptic density protein PSD-95. Science 1995;269: 1937–40.

52. Bacon KB, Premack BA, Gardner P, Schall TJ. Activation of dual T cell signaling pathways by the chemokine RANTES. Science 1995;269:1727–30.

53. Ludford-Menting M, Thomas S, et al. A functional interaction between CD46 and DLG4. J Biol Chem 2002;277:4477–84.

54. Azim A, Knoll J, Marfatia S, Peel D, Bryant P, Chishti A. DLG1: chromosome location of the closest human homologue of the *Drosophila* discs large tumor suppressor gene. Genomics 1995;30:613–6.

55. Ohshiro T, Yagami T, Zhang C, Matsuzaki F. Role of cortical tumour-suppressor proteins in asymmetric division of *Drosophila* neuroblast. Nature (Lond) 2000;408:593–6.

56. Peng C, Manning L, Albertson R, Doe C. The tumour-suppressor genes Igl and Dlg regulate basal protein targeting in *Drosophila* neuroblasts. Nature (Lond) 2000;408:596–600.

57. Ning K, Pei L, Liao M, et al. Dual neuroprotective signaling mediated by down-regulating two distinct phosphatase activities of PTEN. J Neurosci 2004;24: 4052–60.

58. Yanai H, Satoh K, Matsumine A, Akiyama T. The colorectal tumour suppressor APC is present in the NMDA-receptor-PSD-95 complex in the brain. Genes Cells 2000;5:815–22.

N-Methyl-d-Aspartate Receptor Type 2B Is Epigenetically Inactivated and Exhibits Tumor-Suppressive Activity in Human Esophageal Cancer

Myoung Sook Kim, Keishi Yamashita, Jin Hyen Baek, et al.

Cancer Res 2006;66:3409-3418.